Metallography, Microstructure, and Analysis (2023) 12:662–671
https://doi.org/10.1007/s13632-023-00978-8

PEER-REVIEWED PAPER

Microstructure and Mechanical Properties of Ti-Cu-Based Materials Produced by Using Reactive Melt Infiltration and Liquid Phase Sintering Techniques

Husain Rajab Husain Hraam[1] · Serkan Islak[2] · Abdualkarim Musbah M. Gariba[3]

Received: 2 February 2023 / Accepted: 25 May 2023 / Published online: 12 June 2023

Abstract

In the present study, Ti-Cu-based alloys were provided by the simultaneous application of both reactive melt infiltration and liquid phase sintering techniques. In order to apply the reactive melt infiltration technique, stearic acid was added at 10, 15, and 20% by weight as the pore forming agent in titanium. Cold-pressed samples were subjected to two different sintering temperatures (1100 and 1200 °C), and melt copper was provided to leak between the titanium particles, natural pores, and the pores forming upon the vaporization of stearic acid. According to the microstructure results, two types of microstructure (eutectoid and hypereutectoid) formed. Eutectoid structure consists of formation of α-Ti + Ti_2Cu. The presence of Ti_2Cu intermetallic phase caused an increase in hardness. While the increase in the sintering temperature increased transverse rupture strength, the increased amount of copper caused a decrease due to pore formation (natural pores and pores produced). According to the morphology of the surface of fracture, brittle transgranular and partially ductile fractures occurred in the samples. In summary, it was found that 20% Cu amount and 1200 °C were the most suitable in terms of hardness and relative density, while pure titanium had the highest TRS value at 1200 °C.

Keywords Titanium · Copper · Reactive melt infiltration · Liquid phase sintering

Introduction

In recent years, research and development studies on titanium and titanium-based alloys have attracted great interest. Titanium-based materials that are developed by combining their unique properties together are widely used in various fields. Titanium and titanium-based alloys have high specific strength, excellent corrosion resistance, and an extraordinary biocompatibility among the metal materials. However, due to the high chemical reactivity at high temperatures and high melting temperature, it is accepted as one of the metals harder to process. Decreasing the fusion temperature and high reactivity is one of the possible ways to overcome the challenges [1].

Depending on the temperature, titanium is crystallized in two main structures and this provides opportunities to design various combinations of microstructures and thus, enables the adjustment of mechanical properties of Ti. In particular, Ti atoms place themselves in α-Ti having hexagonal close-packed (HCP) crystal structure under room temperature. Conversely, Ti transforms into a β-Ti having body-centered cubic (BCC) crystal structure when the critical transformation temperature (882 ± 2 ℃) is exceeded by increasing the temperature [2]. Alloying elements added to titanium are divided into different classes as neutral, α and β stabilizers according to their effectiveness on the transition temperature of 882 ± 2 ℃. In general, titanium alloys show three microstructure types: α, α + β and β alloys [3, 4]. Copper (Cu) is quite attractive due to high damping capacity, high thermal and electrical conductivity, low density, and good corrosion resistance. Ti-based alloy and Cu combination provide a material group known as Ti-Cu binary alloys [5, 6].

✉ Serkan Islak
serkan@kastamonu.edu.tr

1 Department of Mechanical Engineering, Faculty of Engineering, Elmergib University, Al-Khoms, Libya

2 Department of Mechanical Engineering, Faculty of Engineering and Architecture, Kastamonu University, Kastamonu 37150, Turkey

3 Department of Mechanical Engineering, Higher Institute of Science and Technology, Al-Khoms, Libya

Binary phase diagram of Ti-Cu alloys shows that addition of more than 3% copper element into the titanium alloy will enable to have two phases forming an acicular structure that can improve the mechanical properties of the material and forms the Ti_2Cu phase [7, 8]. Depending on the copper content in the Ti-Cu phase diagram given in Fig. 1, Ti-Cu alloys can show different microstructures such as eutectoid, hypereutectoid, and hypoeutectoid microstructures and enables to adjust the mechanical behaviors of Ti-Cu alloys by controlling the Ti_2Cu precipitation ratio and distribution [1, 9, 10]. Mechanical behavior of Ti alloys is based on the microstructure properties and type of the alloy elements. Intermediate phase, forming the eutectoid structure with α-Ti, is defined as the Ti_2Cu phase that can improve the mechanical properties of the materials. As the Cu content increases, intermetallic Ti_2Cu phase precipitation in Ti alloy also increases. Wang et al., [11] examined the optimization of the mechanical property of Ti-Cu alloy. The results showed that α-Ti + Ti_2Cu-microstructure Ti-Cu alloys exhibited the best ductility than α-Ti + transformed β-Ti and other Ti-Cu alloys with fully transformed microstructure and meanwhile, since increased rate of Ti_2Cu caused both solid solution hardening and precipitation hardening, increased rate of Cu content significantly contributed to decrease in ductility. Takahashi et al., [12] and Ohkubo et al., [13] specified that the increase in the strength, hardness, and wear resistance of titanium alloy is both related to the ageing process and then the precipitation of a large number of Ti_2Cu intermetallic compounds. Sun et al., [14] expressed that as a result of the decomposition of β phase into α-Ti and Ti_2Cu phases in Ti-2.5Cu alloy, it increased the hardness of the Ti_2Cu intermetallic phase alloy in the structure. Morphology and distribution of Ti_2Cu has a significant share in the mechanical property of the titanium alloy containing Cu.

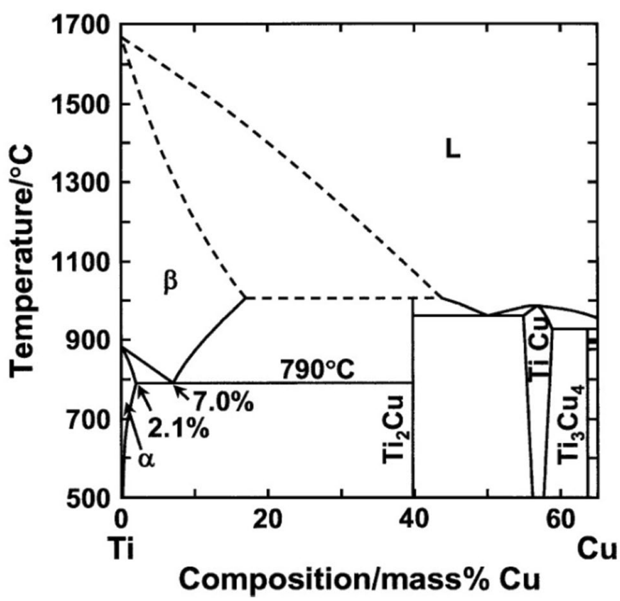

Fig. 1 Ti-Cu phase diagram [1]. Reprinted from Dental Materials, Volume 19, Masafumi Kikuchi, Yukyo Takada, Seigo Kiyosue, Masanobu Yoda, Margaret Woldu, Zhuo Cai, Osamu Okuno, Toru Okabe, Mechanical properties and microstructures of cast Ti–Cu alloys, pg. 174–184, Copyright 2003, with permission from Elsevier

Liquid phase sintering (LPS) is defined as sintering involving liquid and solid coexisting during part or all of the sintering cycle. The presence of a liquid phase between the particles leads to capillary forces that can result in condensation and allows the solid to dissolve and then precipitate away from areas of high surface energy. Condensation rates can therefore be greatly increased by the presence of a liquid [15]. The reactive melt infiltration (RMI) technique is based on the infiltration of porous matrices by melting the active phase or precursor. The prerequisite is that the melting point of the infiltrated material is lower than that of the base material and that the base material is porous. Here, the molten infiltrate material must wet the base material. The melt is attracted by the pores of the base material by capillary forces and the pore volume is completely filled [16].

Numerous production techniques such as mixing casting/vortex method, powder metallurgy (PM), and infiltration are used to manufacture Ti-Cu-based alloys. In the present study, Ti-Cu-based alloys were produced at 1100 °C and 1200 °C by using the RMI and LPS techniques from the PM methods in order to obtain two typical microstructures as eutectoid and hypereutectoid. Some properties of the materials produced were experimentally investigated.

Experimental Studies

The aim of the experimental studies includes application of the RMI and LPS for the production of binary Ti-Cu alloy via PM method. In the study, commercial pure titanium (Ti) powder (particle size − 90 + 22 µm, 99.6% purity) and pure Cu powder (particle size < 45 µm, 99.7% purity) were used. Figure 2 shows the SEM-EDS and XRD analyses of the Ti and Cu powders. While Ti powder had an irregular morphology, Cu powders had a dendritic structure. Elemental α-Ti and Cu phases were detected in XRD analyses of both powders and these results represent the powders used in the present study. Zinc stearate was used as pore-forming agents (PFA) and

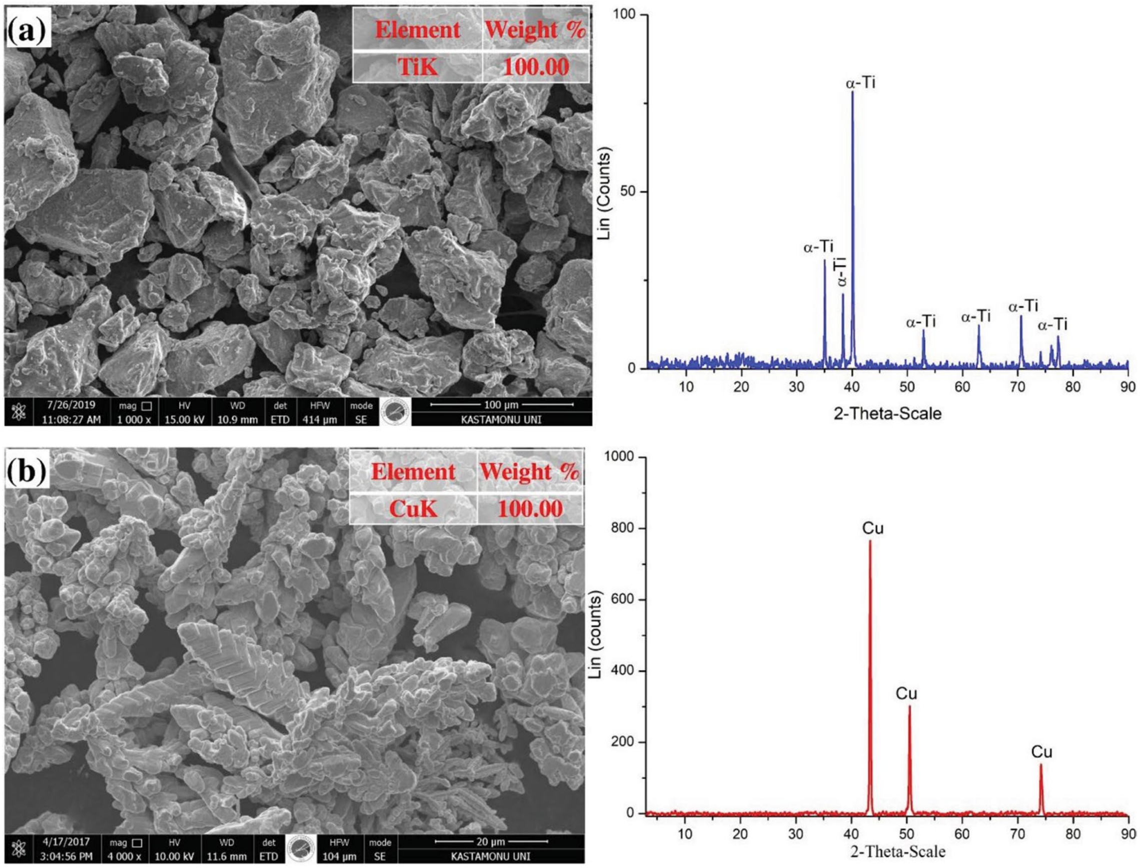

Fig. 2 SEM-EDS and XRD analyses of powders: (**a**) Ti and (**b**) Cu

Ti powder was used as the substrate essential alloy which was mixed and blended at three concentrations (10, 15, and 20%), and the aim of the process was to perform the RMI process. Also, copper powder was used at three different concentrations (10, 15 and 20%) within titanium for LPS process. Then, it is cold-pressed in molds having desired sizes. Cold pressing was carried out using a SPECAC GS15011 brand and model hydraulic press. Ti powder is infiltrated with melt Cu and sintered for 60 minutes at 1100 and 1200 °C under argon atmosphere. RMI and LPS processes were carried out simultaneously in a PROTHERM PTF 18/50/300 brand and model high temperature tube furnace. Finally, microstructural, fracture surface morphology, and mechanical characterization of Ti-Cu alloy is performed. The sample design is given in Fig. 3. The reason behind why the rate of PFA and the rate of copper added for LPS were the same was the infiltration of copper at the same rate into pores formed by PFA. The samples designed were divided in four groups.

Group 1: Ti

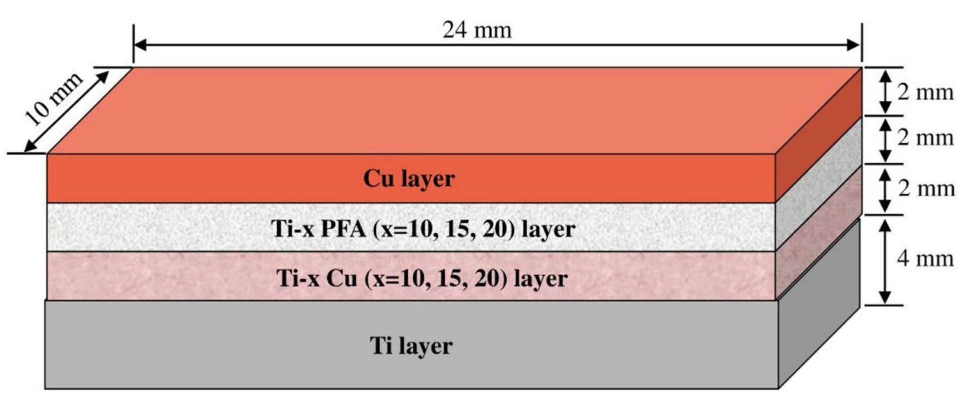

Fig. 3 Sample design

Group 2: Ti/Ti + 10 wt.% Cu/Ti + 10 wt.% PFA/Cu
Group 3: Ti/Ti + 15 wt.% Cu/Ti + 15 wt.% PFA/Cu
Group 4: Ti/Ti + 20 wt.% Cu/Ti + 20 wt.% PFA/Cu

Microstructure and fracture surface characterization were examined by using the found optical microscope (OM) (Olympus GX41 microscope) and a scanning electron microscope (SEM) (FEI QUANTA 250 FEG) equipped with an energy dispersive X-ray spectrometry (EDS). In order to get more detailed information from the sample surface, SE mode was used in SEM. Phase identification was carried out by X-ray diffraction (XRD) (RIGAKU ULTRA IV) equipped with CuK_{α} ($\lambda = 1.54056$ Å) radiation as a source operated at 30 kV and 20 mA between 3 and 90° at a step size of 0.03°. Hardness measurements were performed in SHIMADZU HMV-G21 model micro hardness device by using a load of 1 kg and the dwell time was determined as 16 seconds. Three different areas were selected along the thickness section of the samples and the results are the mean value for each area with standard deviation. In order to detect the transverse rupture strength (TRS), three-point bending test was performed at a test speed of 1 mm/minute by using SHIMADZU universal tensile device with a capacity of 50 kN, under room temperature. Three-point bending test was performed three times for each group. The TRS results obtained were averaged. Experimental densities were calculated according to the Archimedes' principle. A precision balance with the given density kit was used. Relative densities were calculated by using the measured density/theoretical density ratio.

Results and Discussion

XRD analysis was conducted to determine whether or not a new phase is formed between the titanium and copper metals and to obtain information about the presence of oxide. Figure 4 shows the Ti-Cu alloys sintered at 1100 °C and 1200 °C and XRD models of the titanium materials, respectively. Ti_2Cu, α-Ti and Cu phases were detected in the microstructure exclude for the pure titanium sample at both temperature values. Cu phase showed that there is some amount of Cu that did not react. It was understood from the XRD graphics that the density of Ti_2Cu peak increased with the increasing the Cu content (excluding 15% PFA) for 1100 °C. In the study of Xu et al., [8] regarding the mechanical and tribological properties of Ti-Cu alloys, they reported that the rate of Ti_2Cu intermetallic phase increased depending on the increased rate of Cu. When the process temperature increased to 1200 °C, the peak intensity of the phases generally increased due to crystallization. The increase in the phases formed in the samples at the processing temperature of 1200 °C was not at the same angles, but there were increases at different angles. Dong et al., [17] detected the Cu, Ti_2Cu, and α-Ti phases in the microstructure of Ti-Cu alloys produced by the spark plasma sintering. This result is compatible with the present study.

Figure 5 shows the OM images for Ti-Cu samples produced at 1100 °C. In these structures, primary α-Ti (light colored phase) and Ti_2Cu (dark colored phase) intermetallic phases which formed at both particles and the particle boundaries by dispersing some closed spherical pores, precipitated [1]. In the present study, the samples were slowly cooled at the furnace (10 °C/min). Following the slow cooling, the decomposition of the β phase triggered the formation of α phase or the eutectoid structure. The slower the cooling rate, the more eutectoid reactions occur. Also, eutectoid reaction of Ti-Cu alloy is so active, β-Ti phase could not form due to the rapid diffusion of Cu to Ti [18]. Due to this reason, eutectoid reaction caused the precipitation of Ti_2Cu throughout the crystal border of α-Ti during the

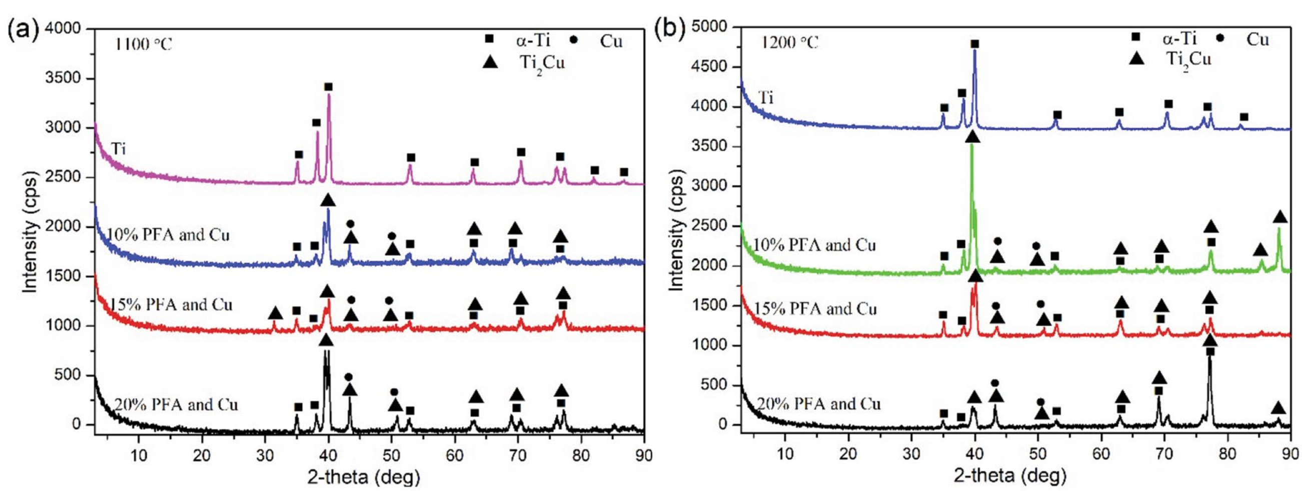

Fig. 4 XRD patterns of samples: (**a**) 1100 °C and (**b**) 1200 °C

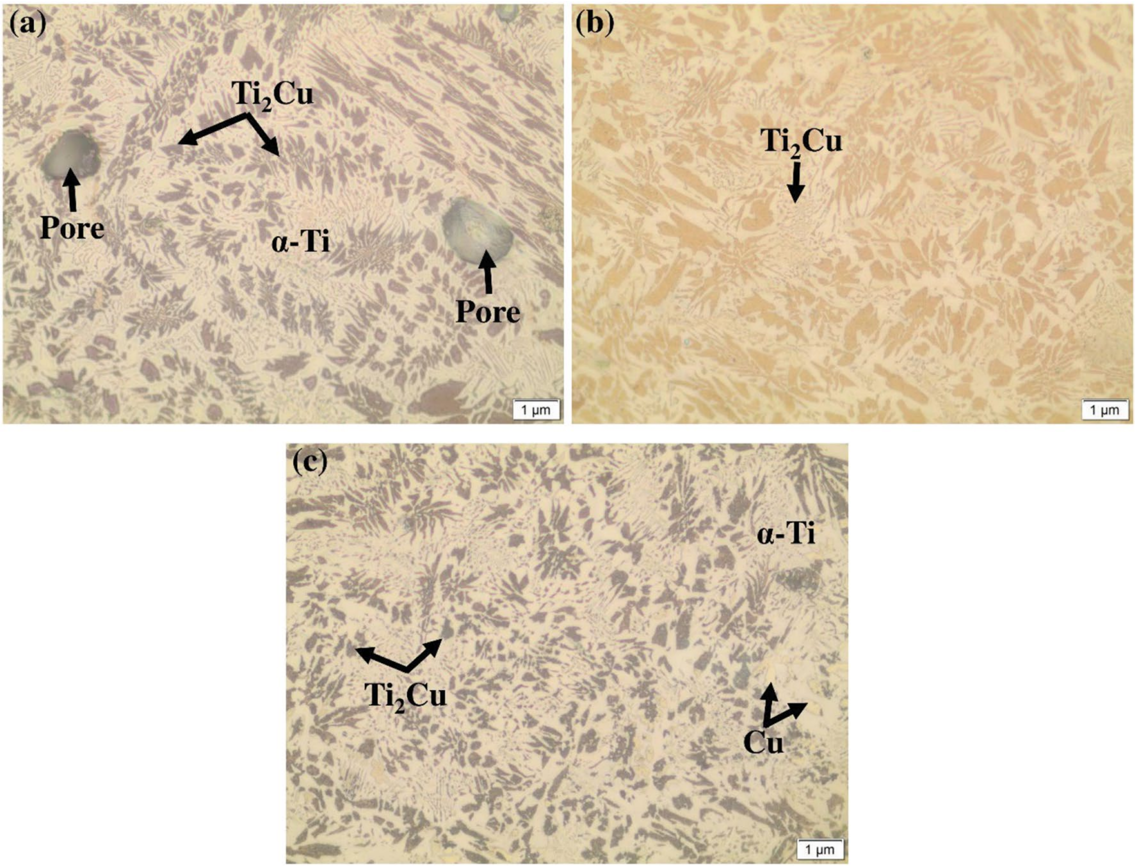

Fig. 5 OM images of samples sintered at 1100 ℃: (**a**) 10 %PFA and Cu, (**b**) 15% PFA and Cu and (**c**) 20 %PFA and Cu

cooling process [19]. The microstructure seen at different PFA and Cu ratios was α-Ti and Ti_2Cu intermetallic.

Figure 6 shows the OM images of Ti-Cu alloys with different PFA and Cu contents that were sintered at 1200 °C. The microstructure seen at 10% PFA and Cu was α-Ti and Ti_2Cu. While α-Ti appears as a light colored phase, Ti_2Cu appears in the form of thin long particles in dark color. Ti_2Cu intermetallic phase became more significant by increasing the infiltrated Cu. At 15% PFA and Cu, a hypereutectoid structure occurred in which layered structures together with Ti_2Cu intermetallic phases were present. While Cu infiltrated at 20% PFA and Cu increased and the layered structure was shown with a dark color, Ti_2Cu (out-of-eutectoid) precipitate was shown with a bright phase.

Figures 7 shows the SEM images of Ti-Cu alloys sintered at 1100 and 1200 °C with different PFA and Cu contents, respectively. As seen in all the SEM images, many bright colored (Ti_2Cu) intermetallic phases with lamellar and dendritic structures precipitated in α-Ti corresponding to the dark phases formed. In addition, the typical lamellar microstructure for slow cooling was seen above the temperature of transition from the α phase to the β phase, regardless of the Cu infiltration content. As the sintering temperature increases, dendritic and lamellar structure became more significant.

Figure 8 shows the hardness measurements for the Ti-Cu alloy samples processed at 1100 and 1200 °C. The interface zone is the zone formed by the LPS process. The infiltration zone is the zone formed by the RMI process. The substrate consists entirely of Ti. Hardness values increased by the increasing rate of Cu and process temperature. Hardness of pure Ti varied between 182 and 242 HV_1 depending on the sintering temperature, while the hardness values of Ti-Cu alloys were between 219 and 343 HV_1 depending on sintering temperature and additional amount of Cu and this value was higher than pure titanium. Gariba et al. [20] in their study on Ti-matrix functionally gradient materials (FGMs), they reported that the matrix had a value of approximately 191 HV. This value is consistent with our study. Generally, the higher the copper amount, the higher the hardness of

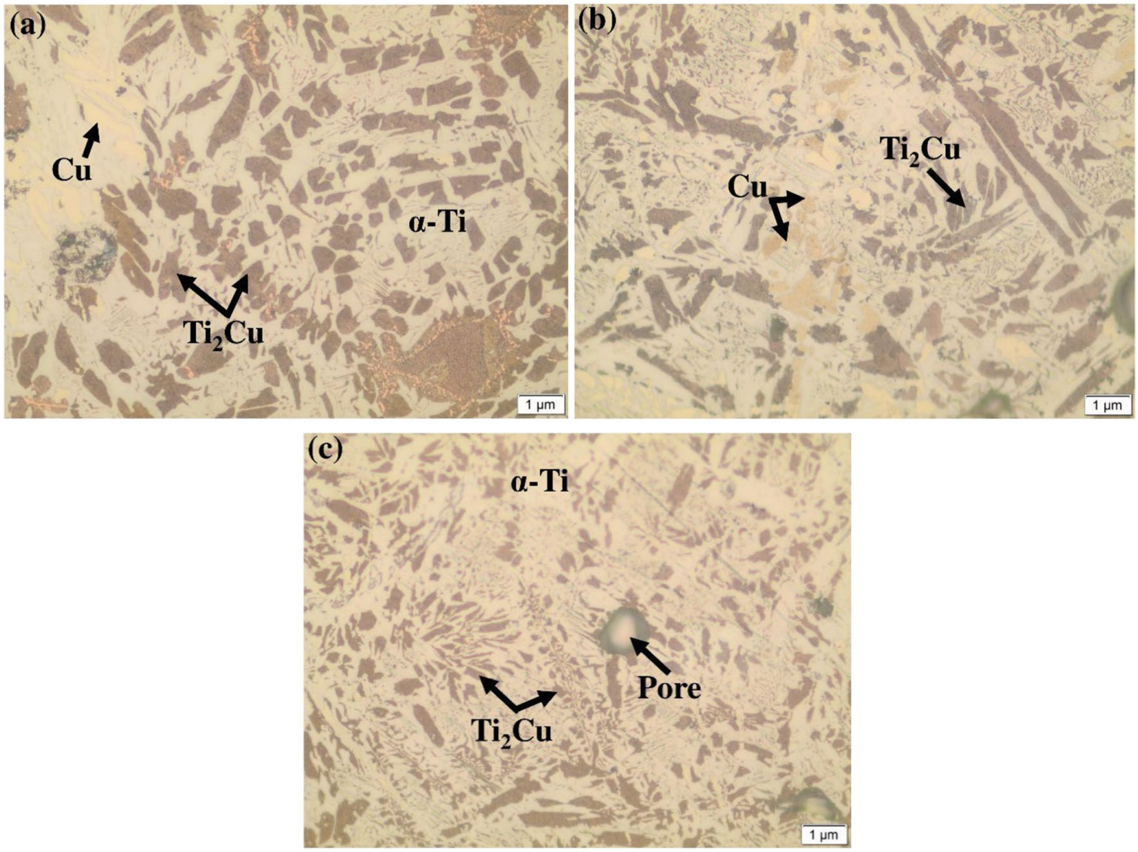

Figure 6 OM images of samples sintered at 1200 ℃: (**a**) 10 %PFA and Cu, (**b**) 15% PFA and Cu and (**c**) 20 %PFA and Cu

the Ti-Cu alloy and this is associated with the increase in hard phase of Ti_2Cu. The increase in hardness occurs due to solid solution hardening of the α-Ti phase and intensification of precipitation by the presence of Ti_2Cu. This mechanism inhibits the movement of dislocations and thus, increases the hardness of Ti-Cu alloy. Increase in hardness by the increasing Cu content is compatible with the findings of Kikuchi et al., [1]. They stated that Ti_2Cu precipitates can strengthen the Ti alloy. In addition, Sun et al. [14] stated that nano-Ti_2Cu precipitates inhibited the dislocation movement and thus, increased the mechanical property. Luangvaranunt and Pripanapong [21] examined some of the properties of Ti-Cu alloys and found the results that are compatible with the hardness stated in the present study.

Table 1 shows the theoretical, experimental, relative densities, and pore ratios of Ti-Cu alloys. When melt copper was infiltrated to titanium, an increase in experimental densities occurred. This can be explained by the fact that the density of copper was higher than titanium. Also, significant increases were seen in densities by the increase in process temperature. An increase in approximately 7.9% occurred in density than pure titanium when 20% Cu was added at 1100 °C. This increase was about 9% at 1200 °C. When copper was added into pure titanium, relative densities of the samples decreased. There was an increase in relative densities due to the increasing rate of copper in copper-containing samples. As in the densities, increases also occurred in the relative densities by the increase in process temperature. Islak et al., [22] specified that as the sintering temperature increased, relative densities increased and pore amount decreased. Alshammari et al., [23] reported that an increase was detected in the Ti-Cu alloys by the increase in the copper rate (89.2–93.4%). In the present thesis study, the pore rates decreased with the increased process temperature. Min et al., [24] stated that the decrease in porosity by the increase in the sintering temperature and the formation of a denser structure were associated with the increase in the diffusion rates.

Figure 9 shows the TRS result of Ti-Cu alloys. The results showed that TRS values of pure Ti and Ti-Cu alloys increased by the increasing sintering temperature. This is because in case of high temperature, there was a good

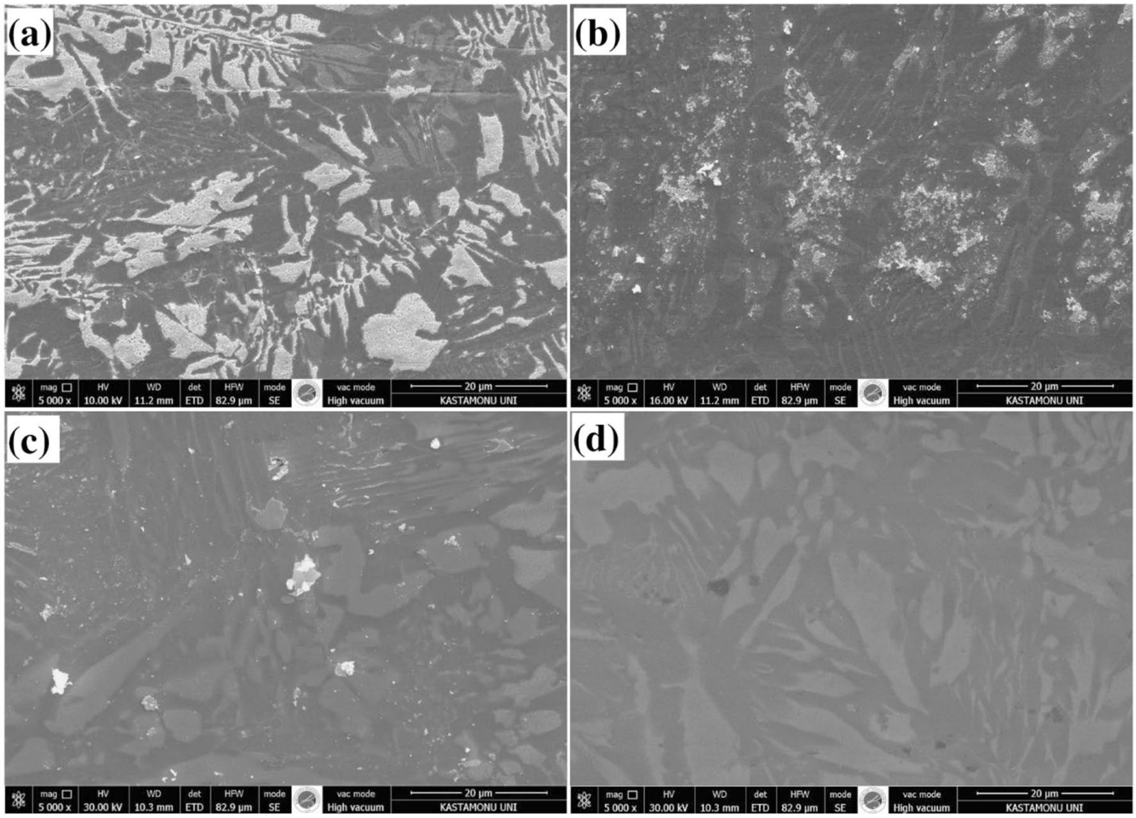

Fig. 7 SEM images of samples: (**a**) 10% PFA and Cu at 1100 °C, (**b**) 15% PFA and Cu at 1100 °C, (**c**) 10% PFA and Cu at 1200 °C and (**d**) 15% PFA and Cu at 1200 °C

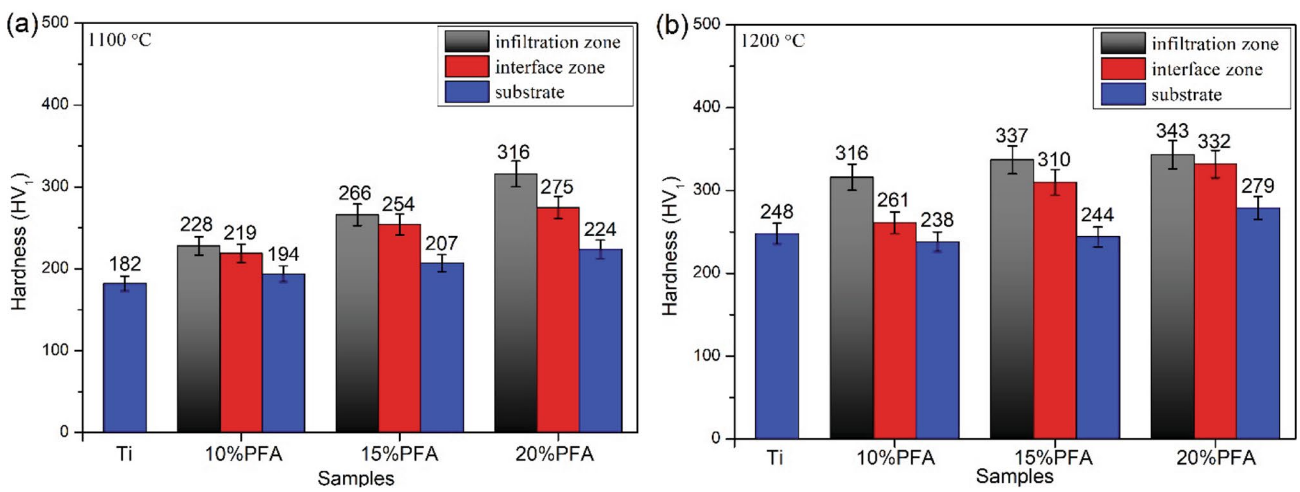

Fig. 8 Micro-hardness values of the samples: (**a**) 1100 °C and (**b**) 1200 °C

binding between the particles. When compared to Ti-Cu alloys, the increase in the TRS value of the base material of pure Ti was a result of the increase in the hardness levels in Ti-Cu alloys and the effect of porosity. In fact, the presence of Ti_2Cu precipitation particles in Ti-Cu alloy increased hardness to a great extent and decreased the ductility of the final alloy. As Cu rate increases, the type of fracture was transformed from ductile fracture to brittle fracture. TRS values of Ti-Cu alloys increased with the increasing sintering temperatures. This is because the good bonding between

Table 1 Densities and pore rates

Samples	Theoretical density, gr/cm^3	Experimental density, gr/cm^3		Relative density, %		Amount of porosity, %	
		1100 °C	1200 °C	1100 °C	1200 °C	1100 °C	1200 °C
Pure Ti	4.51	4.41	4.44	97.8	98.4	2.2	1.6
10% PFA and Cu	4.73	4.43	4.53	93.7	95.8	6.3	4.2
15% PFA and Cu	4.84	4.57	4.66	94.4	96.3	5.6	3.7
20% PFA and Cu	4.96	4.76	4.85	96.0	97.8	4.0	2.2

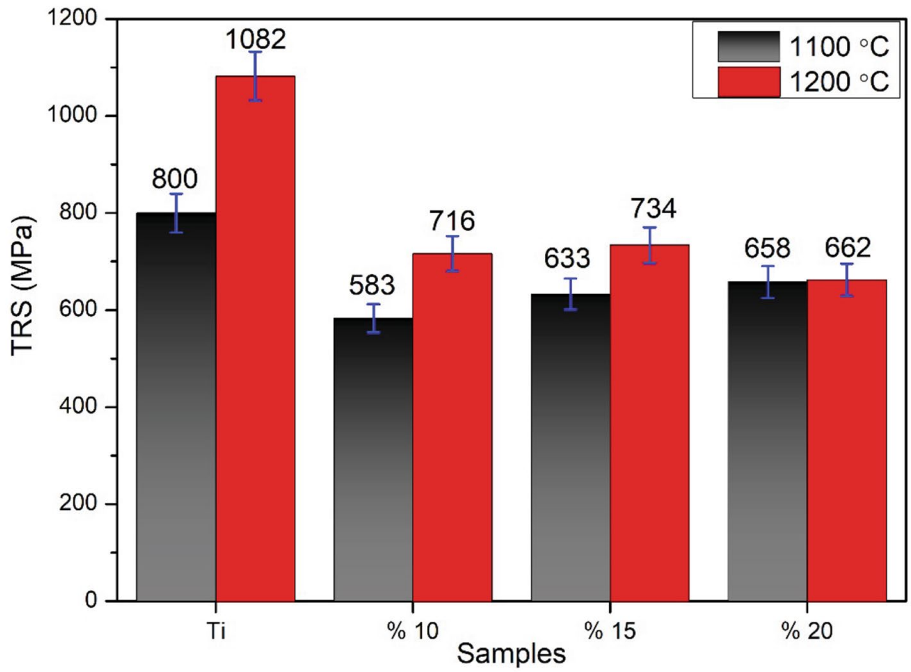

Fig. 9 Effect of sintering temperature and Cu content on TRS

the particles in case of high temperature and the decrease in the pore amount with increased sintering temperature.

Figure 10 shows the macro- and micro-images of the fracture surfaces of samples with 10% PFA and Cu processed at 1100 and 1200 ℃. Upper section represents the region subjected to RMI and LPS process (Fig. 10b). This surface included mostly ductile fracture associated with the presence of numerous cavities mostly caused by Cu effect and brittle fracture mechanisms caused by the presence of Ti_2Cu [25]. Bolzoni et al., [26] in their study on the development of Ti-Cu-Fe alloys produced by powder metallurgy, they emphasized that the presence of Ti_2Cu phase causes brittle fracture. Figure 8c shows the macro-photographs of the samples sintered at 1200 °C. The number of pores decreased more in this structure according to the structures at 1100 °C. As temperature increased, copper became more fluid and leaked into the pores better. Figure 10d shows the upper region of fracture surface analysis of Ti-Cu alloy having 10% PFA and Cu concentration sintered at 1200 °C. Brittle fracture with traces in the form of a river formation and ductile fracture having equiaxial dimples represent the fracture surface. Kompo et al., [27] in their study on the microstructure and mechanical properties of Ti-Cu alloys produced by semi-solid process, reported that the fracture surfaces of the samples generally exhibit brittle fracture behavior and dimples representing ductile fracture were formed on the fractured surface.

Conclusion

The results obtained from the study are given below:

- As the copper concentration increased, two types of micro-structures (eutectoid and hypereutectoid) were found in the Ti-Cu alloys. Eutectoid structure formed of α-Ti and Ti_2Cu phases given in the binary phase diagram.
- According to the results of the XRD analysis, α-Ti, Cu and intermetallic Ti_2Cu phases were detected in the structure. By the increase in the Cu amount, the rate of Ti_2Cu intermetallic phase increased.

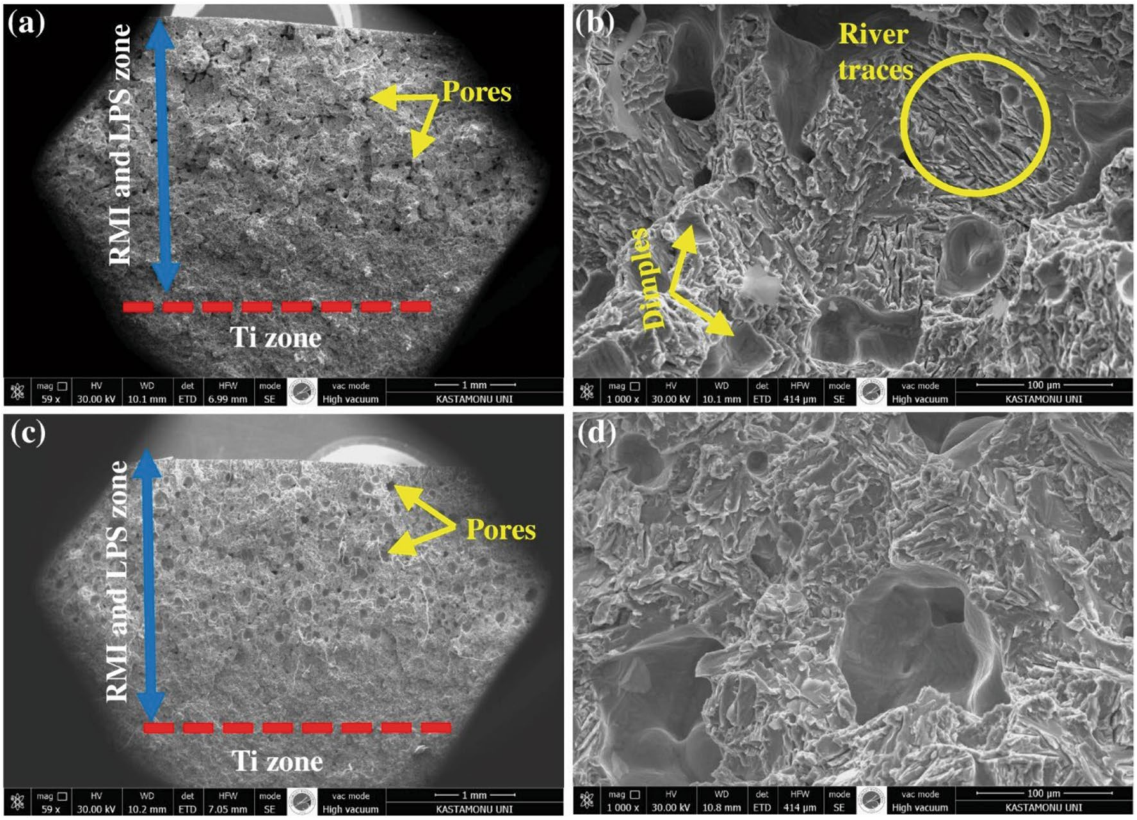

Fig. 10 SEM photographs of fracture surfaces of samples with 10% PFA and Cu: (**a**) 1100 °C, (**b**) upper region of "a," (**c**) 1200 °C and (**d**) upper region of "c"

- Significant increases occurred in hardness by the increase in the sintering temperature and copper content. This was associated with the presence of the intermetallic phase.
- TRS values of pure Ti and Ti-Cu alloys increased by the increasing process temperature. When compared to Ti-Cu alloys, the increase in the TRS value of the base material of pure Ti was a result of the increase in the hardness levels in Ti-Cu alloys and the effect of porosity.

References

1. M. Kikuchi, Y. Takada, S. Kiyosue, M. Yoda, M. Woldu, Z. Cai, O. Okuno, T. Okabe, Mechanical properties and microstructures of cast Ti-Cu alloys. Dent. Mater. **19**, 174–181 (2003). https://doi.org/10.1016/S0109-5641(02)00027-1
2. C. Leyens, M. Peters, *Titanium and titanium alloys: fundamentals and applications* (John Wiley & Sons, USA, 2003) https://doi.org/10.1002/3527602119
3. Y.M. Ahmed, K.S.M. Sahari, M. Ishak, B.A. Khidhir, Titanium and its alloy. Int. J. Sci. Res. **3**, 1351–1361 (2014)
4. Y. Alshammari, F. Yang, L. Bolzoni, Yield of binary Ti-Cu and Ti-Mn alloys produced via powder metallurgy. Appl. Mech. Mater. **884**, 49–57 (2018). https://doi.org/10.4028/www.scientific.net/AMM.884.49
5. Y. Takada, O. Okuno, Corrosion characteristics of α-Ti and Ti_2Cu composing Ti-Cu alloys. Dent. Mater. J. **24**, 610–616 (2005). https://doi.org/10.4012/dmj.24.610
6. X. Yao, Q.Y. Sun, L. Xiao, J. Sun, Effect of Ti_2Cu precipitates on mechanical behavior of Ti-2.5 Cu alloy subjected to different heat treatments. J. Alloys Compd. **484**, 196–202 (2009). https://doi.org/10.1016/j.jallcom.2009.04.095
7. S.M. Javadhesari, S. Alipour, M.R. Akbarpour, Biocompatibility, osseointegration, antibacterial and mechanical properties of nanocrystalline Ti-Cu alloy as a new orthopedic material. Colloids Surf. B Colloid Surf. B. **189**, 110889 (2020). https://doi.org/10.1016/j.colsurfb.2020.110889
8. Y. Xu, J. Jiang, Z. Yang, Q. Zhao, Y. Chen, Y. Zhao, The effect of copper content on the mechanical and tribological properties of hypo-hyper-and eutectoid Ti-Cu alloys. Materials. **13**, 3411 (2020). https://doi.org/10.3390/ma13153411
9. H. Paul, R. Chulist, M.M. Miszczyk, G. Cios, A. Galka, W. Skuza, P. Petrzak, I. Mania, Interfacial reactions and structural properties of explosively welded titanium/copper plates. IOP Conf. Ser. Mater. Sci. Eng. **770**, 012033 (2020). https://doi.org/10.1088/1757-899X/770/1/012033
10. C.D. Bohórquez, S.P. Pérez, A. Sarmiento, M.E. Mendoza, Effect of temperature on morphology and wear of a Cu-Ti-TiC MMC sintered by abnormal glow discharge. Mater. Res. Express. **7**, 026501 (2020). https://doi.org/10.1088/2053-1591/ab6e3b
11. J. Wanga, S. Zhang, Z. Sun, H. Wang, L. Ren, K. Yang, Optimization of mechanical property, antibacterial property and corrosion resistance of Ti-Cu alloy for dental implant. J. Mater. Sci.

Technol. **35**, 2336–2344 (2019). https://doi.org/10.1016/j.jmst.2019.03.044
12. M. Takahashi, M. Kikuchi, Y. Takada, O. Okuno, Mechanical properties and microstructures of dental cast Ti-Ag and Ti-Cu alloys. Dent. Mater. J. **21**, 270–280 (2002). https://doi.org/10.4012/dmj.21.270
13. C. Ohkubo, I. Shimura, T. Aoki, S. Hanatani, T. Hosoi, M. Hattori, Y. Oda, T. Okabe, Wear resistance of experimental Ti-Cu alloys. Biomaterials. **24**, 3377–3381 (2003). https://doi.org/10.1016/S0142-9612(03)00157-1
14. Q.Y. Sun, Z.T. Yu, R.H. Zhu, Dynamic fracture toughness of Ti-2.5 Cu alloy strengthened with nano-scale particles at room and low temperatures. Mater. Sci. Eng. A. **483**, 131–134 (2008). https://doi.org/10.1016/j.msea.2006.11.171
15. S.H. Huo, M. Qian, G.B. Schaffer, E. Crossin, (2011) Aluminium powder metallurgy. In: Fundamentals of Aluminium Metallurgy, Woodhead Publishing Series in Metals and Surface Engineering, 655-701 (2011), https://doi.org/10.1533/9780857090256.3.655
16. P.E. de Jongh, T.M. Eggenhuisen, Melt infiltration: an emerging technique for the preparation of novel functional nanostructured materials. Adv. Mater. **25**(46), 6672–6690 (2013). https://doi.org/10.1002/adma.201301912
17. R. Dong, W. Zhu, C. Zhao, Y. Zhang, F. Ren, Microstructure, mechanical properties, and sliding wear behavior of spark plasma sintered Ti-Cu alloys. Metall. Mater. Trans. A. **49**, 6147–6160 (2018). https://doi.org/10.1007/s11661-018-4953-0
18. O. Taguchi, Y. Iijima, Diffusion of copper, silver and gold in α-titanium. Philos. Mag. A. **72**, 1649–1655 (1995). https://doi.org/10.1080/01418619508243935
19. C.B. Yi, Z.Y. Ke, L. Zhang, J. Tan, Y.H. Jiang, Z. He, Antibacterial Ti-Cu alloy with enhanced mechanical properties as implant applications. Mater. Res. Express. **7**, 105404 (2020). https://doi.org/10.1088/2053-1591/abc371
20. A.M.M. Gariba, S. Islak, H.R.H. Hraam, M. Akkaş, Microstructural and mechanical properties of Ti-B4C/CNF functionally graded materials. Metallogr. Microstruct. Anal. **11**, 736–745 (2022). https://doi.org/10.1007/s13632-022-00900-8
21. T. Luangvaranunt, P. Pripanapong, Pin-on-disc wear of precipitation hardened titanium–copper alloys fabricated by powder metallurgy. Mater. Trans. **53**, 518–523 (2012). https://doi.org/10.2320/matertrans.M2011293
22. S. Islak, Ö. Küçük, Ö. Eski, C. Özorak, M. Akkaş, The effect of CNT content and sintering temperature on some properties of CNT-reinforced MgAl composites. Sci. Sint. **49**, 347–357 (2017). https://doi.org/10.2298/SOS1704347I
23. Y. Alshammari, F. Yang, L. Bolzoni, Low-cost powder metallurgy Ti-Cu alloys as a potential antibacterial material. J. Mech. Behav. Biomed. Mater. **95**, 232–239 (2019). https://doi.org/10.1016/j.jmbbm.2019.04.004
24. K.H. Min, S.P. Kang, D.G. Kim, Y. Do Kim, Sintering characteristic of Al_2O_3-reinforced 2xxx series Al composite powders. J. Alloys Compd. **400**, 150–153 (2005). https://doi.org/10.1016/j.jallcom.2005.03.070
25. H.R.H. Hraam, *Investigation of the microstructure and mechanical properties of titanium-based-material produced by powder metallurgy technique* (Institute of Science Kastamonu University, Turkey, 2021)
26. L. Bolzoni, F. Yang, M. Paul, Development and characterisation of low-cost powder metallurgy Ti-Cu-Fe alloys. J. Mater. Res. Technol. **24**, 2678–2687 (2023). https://doi.org/10.1016/j.jmrt.2023.03.178
27. K.N. Campo, C.C.D. Freitas, É.S.N. Lopes, S.C. Moon, R. Dippenaar, R. Caram, Microstructure and mechanical behavior of Ti-Cu alloys produced by semisolid processing. Trans. Nonferrous Met. Soc. China. **32**(11), 3578–3586 (2022). https://doi.org/10.1016/S1003-6326(22)66040-0